EIGENVALUE DENSITY OF EMPIRICAL COVARIANCE MATRIX FOR CORRELATED SAMPLES*

ZDZISŁAW BURDA, JERZY JURKIEWICZ, BARTŁOMIEJ WACŁAW

Mark Kac Complex Systems Research Centre
and
Marian Smoluchowski Institute of Physics, Jagellonian University
Reymonta 4, 30-059 Kraków, Poland

We describe a method to determine the eigenvalue density of empirical covariance matrix in the presence of correlations between samples. This is a straightforward generalization of the method developed earlier by the authors for uncorrelated samples (Z. Burda, A. Görlich, J. Jurkiewicz, B. Waclaw, `cond-mat/0508341`). The method allows for exact determination of the experimental spectrum for a given covariance matrix and given correlations between samples in the limit $N \to \infty$ and $N/T = r = \text{const}$ with N being the number of degrees of freedom and T being the number of samples. We discuss the effect of correlations on several examples.

PACS numbers: 02.50.–r, 02.60.–x, 89.90.+n

Spectral properties of empirical covariance matrices have been intensively studied for uncorrelated samples [2–4]. The eigenvalue distribution of the empirical covariance matrix is related to the eigenvalue distribution of the true covariance matrix by Marčenko–Pastur equation [2]. This relation plays an important role in many practical problems ranging from physics, telecommunication [5] and information theory [6] to biology and quantitative finance [7]. Recently the corresponding equations has also been derived for correlated samples [8].

We will discuss some practical applications of these equations. More precisely we will show how to use them to explicitly compute the eigenvalue density of the empirical covariance matrix when the true covariance matrix is given. This method is of importance for instance for the problem of optimal portfolio selection if one considers strategies based on the analysis of very

---

* Presented at the Conference on Applications of Random Matrices to Economy and Other Complex Systems, Kraków, Poland, May 25–28, 2005.

short time price changes which are known to be correlated in time, or for problems in telecommunication where one discusses propagation of signal through a random medium from a certain number of senders to a certain number of receivers (see *e.g.* [9] and references therein) and for many other problems.

To set the stage let us briefly recall the mathematical formulation of the problem. Let $\boldsymbol{X} = (X_{i\alpha})$ be a real rectangular matrix of dimension $N \times T$ representing sampled values of a statistical system with N-degrees of freedom obtained in T measurements. α-th column of the matrix $\boldsymbol{X}$ contains N numbers obtained in the α-th measurement. The standard estimator of the covariance matrix $\boldsymbol{C}$, describing correlations the degrees of freedom, is given by the matrix[1] $\boldsymbol{c} = (1/T)\boldsymbol{X}\boldsymbol{X}^{\tau}$: $c_{ij} = (1/T)\sum_{\alpha} X_{i\alpha}X_{j\alpha}$ which is called empirical covariance matrix. $\boldsymbol{X}^{\tau}$ stands for the transpose of $\boldsymbol{X}$. The Marčenko and Pastur solution [2] refers to the situation when the measurements are uncorrelated:

$$\langle X_{i\alpha}X_{j\beta} \rangle = \delta_{\alpha\beta}C_{ij}. \tag{1}$$

It relates the eigenvalue density of $\boldsymbol{c}$ to that of $\boldsymbol{C}$. In the presence of correlations the Kronecker delta is replaced by an arbitrary symmetric semi-positive matrix $\boldsymbol{A}$ describing correlations between measurements:

$$\langle X_{i\alpha}X_{j\beta} \rangle = A_{\alpha\beta}C_{ij}. \tag{2}$$

We shall discuss this case in the present paper. Our aim is to recall the formal solution [8] and to show how to use it to calculate spectral density $\rho_{\boldsymbol{c}}$ of the empirical covariance matrix $\boldsymbol{c}$, for given matrices $\boldsymbol{A}, \boldsymbol{C}$.

The equations for the eigenvalue density $\rho_{\boldsymbol{c}}$ can be derived by assuming that statistical fluctuations in the studied system are Gaussian. Then the matrix $\boldsymbol{X}$ can be treated as a random matrix chosen from the Wishart ensemble with the following probability measure [8, 10]:

$$P(\boldsymbol{X}) \, D\boldsymbol{X} = \mathcal{N} \exp\left[-\frac{1}{2} \operatorname{Tr} \boldsymbol{X}^{\tau} \boldsymbol{C}^{-1} \boldsymbol{X} \boldsymbol{A}^{-1} \right] \prod_{i,\alpha=1}^{N,T} dX_{i\alpha} \, , \tag{3}$$

where the normalization constant is $\mathcal{N} = (2\pi)^{-\frac{NT}{2}}(\det \boldsymbol{C})^{-\frac{T}{2}}(\det \boldsymbol{A})^{-\frac{N}{2}}$. One can easily check that correlations between matrices chosen randomly from this ensemble are given by (2). Applying a diagrammatic technique [11–13] one can calculate averages of various quantities, in particular the resolvent of the empirical covariance matrix:

$$g_{\boldsymbol{c}}(z) = \left\langle \operatorname{Tr} \frac{1}{z - \boldsymbol{c}} \right\rangle = \left\langle \operatorname{Tr} \frac{1}{z - (1/\mathrm{T})\boldsymbol{X}\boldsymbol{X}^{\tau}} \right\rangle . \tag{4}$$

---

[1] We shall assume throughout the paper that $\langle X_{i\alpha} \rangle = 0$.

The brackets denote the average over the ensemble of random matrices $\boldsymbol{X}$ with the probability measure (3). It is convenient to express $g_{\boldsymbol{c}}$ in terms of generating functions for spectral moments of $\boldsymbol{C}, \boldsymbol{A}$ and $\boldsymbol{c}$:

$$M_{\boldsymbol{C}}(z) = \sum_{k=1}^{\infty} \frac{M_{\boldsymbol{C}k}}{z^k}, \quad M_{\boldsymbol{A}}(z) = \sum_{k=1}^{\infty} \frac{M_{\boldsymbol{A}k}}{z^k}, \quad m_{\boldsymbol{c}}(z) = \sum_{k=1}^{\infty} \frac{m_{\boldsymbol{c}k}}{z^k}, \qquad (5)$$

where $M_{\boldsymbol{C}k} = \int \rho_{\boldsymbol{C}}(x) x^k dx$ are spectral moments of the eigenvalue density of the matrix $\boldsymbol{C}$ and similarly $M_{\boldsymbol{A}}$ and $m_{\boldsymbol{c}}$ of $\boldsymbol{A}$ and $\boldsymbol{c}$. The generating functions are related to the corresponding resolvents, in particular $m_{\boldsymbol{c}}(z) = z g_{\boldsymbol{c}}(z) - 1$.

In the limit of $N \to \infty$ and fixed "rectangularity" coefficient $r = N/T$ the generating functions $M_{\boldsymbol{C}}$ and $m_{\boldsymbol{c}}$ are related by two equations [8]:

$$\begin{aligned} m_{\boldsymbol{c}}(z) &= M_{\boldsymbol{C}}(Z), \\ z &= Z r M_{\boldsymbol{C}}(Z) M_{\boldsymbol{A}}^{-1}(r M_{\boldsymbol{C}}(Z)), \end{aligned} \qquad (6)$$

where $M_{\boldsymbol{A}}^{-1}$ is the inverse function of the generating function $M_{\boldsymbol{A}}$. From these equations one can formally calculate $m_{\boldsymbol{c}}(z)$ when $\boldsymbol{A}$ and $\boldsymbol{C}$ are given. The variable Z is auxiliary. Having determined $m_{\boldsymbol{c}}(z)$ from the equations (6) one can calculate the resolvent $g_{\boldsymbol{c}}(z) = (m_{\boldsymbol{c}}(z) + 1)/z$ and the eigenvalue density $\rho_{\boldsymbol{c}}(z)$ of the empirical covariance matrix $\boldsymbol{c}$:

$$\rho_{\boldsymbol{c}}(x) = -\frac{1}{\pi} \text{Im} \, g_{\boldsymbol{c}}(x + i0^+) = -\frac{1}{\pi} \text{Im} \, \frac{1 + m_{\boldsymbol{c}}(x + i0^+)}{x + i0^+}. \qquad (7)$$

Before we show how to calculate $m_{\boldsymbol{c}}(z)$ in the most general case we will first recall the case without correlations that is for $A_{\alpha\beta}$ equal to the Kronecker delta. The equations (6) simplify to [13]:

$$\begin{aligned} m_{\boldsymbol{c}}(z) &= M_{\boldsymbol{C}}(Z), \\ z &= Z(1 + r M_{\boldsymbol{C}}(Z)). \end{aligned} \qquad (8)$$

This set of equations is equivalent to the Marčenko–Pastur equation [2]. It can be directly used to determine the eigenvalue density $\rho_{\boldsymbol{c}}(x)$ [1]. We will sketch the method below. Let $\lambda_1 < \cdots < \lambda_k$ be ordered eigenvalues of C and n_k their multiplicities. The generating function $M_{\boldsymbol{C}}(Z)$ takes the form:

$$M_{\boldsymbol{C}}(Z) = \sum_{k=1}^{K} \frac{p_k \lambda_k}{Z - \lambda_k}, \qquad (9)$$

where $p_k = n_k/N$. Using (8) and (9) we can determine $m_{\boldsymbol{c}}(z)$ and hence from Eq. (7) the eigenvalue density function $\rho_{\boldsymbol{c}}(x)$. The shape of the eigenvalue

density $\rho_{\boldsymbol{c}}(x)$ is encoded in the behavior of the conformal map (8) near the critical horizon [1], defined as a curve on the Z-plane which is mapped by (8) into an interval $[x_-, x_+]$ on the real axis in the z-plane. Here x_-, x_+ denote the upper and the lower edge of the support of the function $\rho_{\boldsymbol{c}}(x)$. The critical horizon may be determined as follows: let $Z = X + iY$ be a point on the horizon. Because the eigenvalues are real the imaginary part of $z = z(Z)$ must vanish. This gives the equation:

$$\sum_k \frac{p_k \lambda_k^2}{(X - \lambda_k)^2 + Y^2} = \frac{1}{r} \, . \tag{10}$$

Solving this equation for $Y = Y(X)$ for given X we find the desired curve giving the critical horizon: $X + iY(X)$. The equation (10) has two symmetric roots $\pm Y$ because of the ambiguity of the map $z = z(Z)$. They can be found numerically by an iterative method taking as an initial value Y_0 a small positive number. The positive root is mapped into $z = x + i0^+$. The corresponding values of $x = z(Z)$ and $\rho_{\boldsymbol{c}}(x)$ are given by:

$$x(Z) = X + r \sum_k p_k \lambda_k + r \sum_k \frac{p_k \lambda_k^2 (X - \lambda_k)}{(X - \lambda_k)^2 + Y^2} \, , \tag{11}$$

and

$$\rho_{\boldsymbol{c}}(Z) = -\frac{Y}{\pi x(Z)} \sum_k \frac{p_k \lambda_k}{(X - \lambda_k)^2 + Y^2} \, . \tag{12}$$

Treating Z as a dummy parameter we obtain a pair $(x, \rho_{\boldsymbol{c}})$ which is equivalent to the eigenvalue density $\rho_{\boldsymbol{c}}(x)$. Briefly speaking, the variable $Z = X + iY$ is used to parametrize both the eigenvalue x and the spectrum $\rho_{\boldsymbol{c}}$.

The variable X is an independent variable in this construction. It is restricted to a finite range $X \in [X_-, X_+]$. The limits of this range are mapped into the lower, x_-, and the upper edge, x_+, of the spectrum $\rho_{\boldsymbol{c}}(x)$. They can be determined numerically by observing that they come from the points where the critical horizon intersects the real axis. Setting $Y = 0$ in Eq. (10) we obtain an equation for X whose largest root corresponds to X_+ and the smallest to X_-. The roots can be found numerically.

The advantage of this method in comparison with the others [3,4] is that one has to solve only one algebraic equation for one point in the spectrum, which can be done either analytically (for $K \leq 4$ or some other special cases) or numerically. A more detailed discussion can be found in [1].

Encouraged by the success of this approach we want to adapt it to the general case of correlated samples (2). We have to return to the equations (6). For given matrix $\boldsymbol{C}$ we can calculate $M_{\boldsymbol{C}}(Z)$ (9) and simi-

larly for $\boldsymbol{A}$:

$$M_{\boldsymbol{A}}(Z') = \sum_{\alpha=1}^{\kappa} \frac{p_{\alpha}\Lambda_{\alpha}}{Z' - \Lambda_{\alpha}} \,. \tag{13}$$

We have indexed the parameters of the spectrum of the matrix $\boldsymbol{A}$ by Greek indices to distinguish them from the parameters of the spectrum of $\boldsymbol{C}$. As before, the first step of the construction is to parametrize critical horizon Z by one real variable. However, the situation is now more complicated because we have to invert $M_{\boldsymbol{A}}$ which may give a multi-valued function. Let us introduce the notation: $Z = X + iY$ and $M_{\boldsymbol{A}}^{-1} = U + iV$. Now, $x(Z) = z(Z)$ takes the form:

$$\begin{aligned}
x \ = \ &r \sum_{k} \frac{p_k \lambda_k \left[U(X^2 + Y^2) + \lambda_k(YV - XU) \right]}{(X - \lambda_k)^2 + Y^2} \\
&+ ir \sum_{k} \frac{p_k \lambda_k \left[V(X^2 + Y^2) - \lambda_k(XV + YU) \right]}{(X - \lambda_k)^2 + Y^2} \,,
\end{aligned} \tag{14}$$

and the condition $x \in R$ implies that

$$F_1(X, Y, U, V) \equiv \sum_{k} \frac{p_k \lambda_k \left[V(X^2 + Y^2) - \lambda_k(XV + YU) \right]}{(X - \lambda_k)^2 + Y^2} = 0 \,. \tag{15}$$

In order to invert $M_{\boldsymbol{A}}$ and to calculate U, V we use the relation $rM_{\boldsymbol{C}}(X + iY) = M_{\boldsymbol{A}}(U + iV)$ which gives:

$$r \sum_{k} \frac{p_k \lambda_k (X - \lambda_k - iY)}{(X - \lambda_k)^2 + Y^2} = \sum_{\alpha} \frac{p_{\alpha}\Lambda_{\alpha}(U - \Lambda_{\alpha} - iV)}{(U - \Lambda_{\alpha})^2 + V^2} \,.$$

Comparing the real and imaginary parts we get:

$$F_2(X, Y, U, V) \ \equiv \ r \sum_{k} \frac{p_k \lambda_k (X - \lambda_k)}{(X - \lambda_k)^2 + Y^2} - \sum_{\alpha} \frac{p_{\alpha}\Lambda_{\alpha}(U - \Lambda_{\alpha})}{(U - \Lambda_{\alpha})^2 + V^2} = 0 \,, \tag{16}$$

$$F_3(X, Y, U, V) \ \equiv \ rY \sum_{k} \frac{p_k \lambda_k}{(X - \lambda_k)^2 + Y^2} - V \sum_{\alpha} \frac{p_{\alpha}\Lambda_{\alpha}}{(U - \Lambda_{\alpha})^2 + V^2} = 0 \,. \tag{17}$$

For fixed X, the set of three equations (15)–(17) has to be solved numerically for three unknown variables Y, U, V. Then we can use formulae (12) and (14) to determine the spectrum $\rho_{\boldsymbol{c}}(x)$, as it was done in the previous case for $\boldsymbol{A} = \boldsymbol{1}$.

These new equations are much more complicated than before and have no such a beautiful graphical interpretation [1] as Eq. (10). One can immediately realize that it is easy to eliminate the variable U from Eq. (15) to obtain a set of two equations for two variables Y, V. This makes however the equations less transparent and does not simplify the calculations.

There are no universal root finding procedures for a nonlinear set of equations. Moreover all of them are usually very sensitive to the choice of the initial condition and therefore it is difficult to guarantee that the procedure will converge to the wanted solution starting from some initial condition unless a special care is payed. In other words we have to make some effort to fully automatize root finding on a desired Riemann sheet. The idea is to use the continuity of the solution as we shall explain below. Rewrite Eqs. (15)–(17) in a compact form:

$$\vec{F}(X, \vec{r}) = 0, \tag{18}$$

where $\vec{r} = (Y, U, V) = (r_1, r_2, r_3)$ and $\vec{F} = (F_1, F_2, F_3)$. Instead of a single equation (10) we have now three equations which must be solved for a 3-vector $\vec{r}$. The solution $\vec{r} = \vec{r}(X)$ is a continuous function of X. For given X different solutions $\vec{r}(X)$ of Eq. (18) which lie on different Riemann sheets assume different values as long as they are outside the real axis. So they can be distinguished by value. Suppose that we know the value $\vec{r} = \vec{r}(X_0)$ for some X_0 and that $(Y(X_0), U(X_0), V(X_0))$ is the desired solution. In order to calculate $\vec{r}$ for $X = X_0 + dX$ we can use the first term of the Taylor series:

$$\vec{r}(X_0 + dX) \cong \vec{r}(X_0) + \left[\frac{d\vec{r}(X)}{dX} \right]_{X=X_0} \cdot dX \tag{19}$$

as an initial point for the root finding procedure. The partial derivatives of $\vec{r}$ with respect to X can be analytically found by differentiating (18) which gives:

$$\frac{d\vec{r}(X)}{dX} = -\boldsymbol{Q} \, \frac{d\vec{F}}{dX}, \tag{20}$$

where $\boldsymbol{Q}$ is the inverse of the matrix $(\partial F_i/\partial r_j)_{ij}$, whose elements can be explicitly calculated from Eqs. (15)–(17). Because of the continuity of the solution this procedure must be convergent to the solution on the same Riemann sheet as for X_0 if dX is small enough. Then we can keep on repeating the whole procedure moving in small steps $X \to X + dX$ along the same solution. The procedure is stopped when $Y \leq 0$ because this means that we have reached the point $\rho_c(x) = 0$. Thus if we can guarantee that $\vec{r}(X_0)$ is on the correct Riemann sheet, all other $\vec{r}(X)$ obtained in this procedure will be on the same sheet. The check, whether $\vec{r}(X_0)$ lies on the desired Riemann sheet, does not have to be very efficient since it is done

once per run or if the spectrum consists of disconnected parts, it should be done as many times as is the number of parts.

Let us remark that the parameter X, being just the real part of Z, which we used here to parametrize the critical horizon is not always well suited to this purpose. In general case one has to use a parameter which uniquely parametrizes the solution. In all the cases discussed below except one, X does the job.

In some cases, where the map between z and Z is known explicitly one can simplify the method. Exponential correlations of samples, which are physically important, belong to this class:

$$A_{\alpha\beta} = \exp\left(-\frac{|\alpha - \beta|}{\tau}\right). \tag{21}$$

In this case an exact formula of the map $z = z(Z)$ is known[2] [8]:

$$z = Z\left(\coth(1/\tau) \cdot r M_{\boldsymbol{C}}(Z) + \sqrt{1 + \frac{r^2}{\sinh(1/\tau)^2} M_{\boldsymbol{C}}^2(Z)}\right), \tag{22}$$

where τ is the range of correlations. In the limit $\tau \to 0$, the quantities $\sinh(1/\tau) \to \infty$, $\coth(1/\tau) \to 1$ and in consequence Eq. (22) simplifies to (8) as it should. Because of the presence of the square root in (22) it is hard to divide the above formula into the real and imaginary part. This is however not a problem for a numerical root finder. Changing X in small steps between the limiting values X_- and X_+ we solve the equation $\mathrm{Im}\,(z(X + iY)) = 0$ for $Y = Y(X)$ and calculate $x = z(X+iY)$ and $\rho_{\boldsymbol{c}}(x)$ by means of the formula (12). The limiting values $X_\pm$ which correspond to the largest and smallest real value on the horizon can be determined by solving the equation $\mathrm{Im}\,(z(X + iY)) = 0$ for X on real axis that is for $Y \to 0^+$.

The influence of the correlation time τ on the map $z = z(Z)$ is illustrated in Fig. 1. Here $\boldsymbol{C}$ has two eigenvalues $\{\lambda_i\} = \{1, 2\}$ with equal weights $p_1 = p_2$. One sees that for small r and for τ being not very large the only effect of increasing τ is similar to increasing r. However, for larger r and growing correlation time the map is deformed. This can be easily explained, because for small $r/\sinh(1/\tau) \ll 1$ the square root in the formula (22) is approximately equal 1. This means that formula (22) reduces to the case (8) without correlations but with new $r' = r \cdot \coth(1/\tau)$. When the ratio $r/\sinh(1/\tau)$ becomes larger the corrections begin to play an important role in the map (22). This observation indicates that the presence of exponential correlations between samples may be confused with pure correlations ($\boldsymbol{C} \neq \boldsymbol{1}, \boldsymbol{A} = \boldsymbol{1}$) but with modified "rectangularity" coefficient r (see Fig. 2).

---

[2] Actually in [8] rather a relation $Z = Z(z)$ is given but it can be easily inverted for $z = z(Z)$.
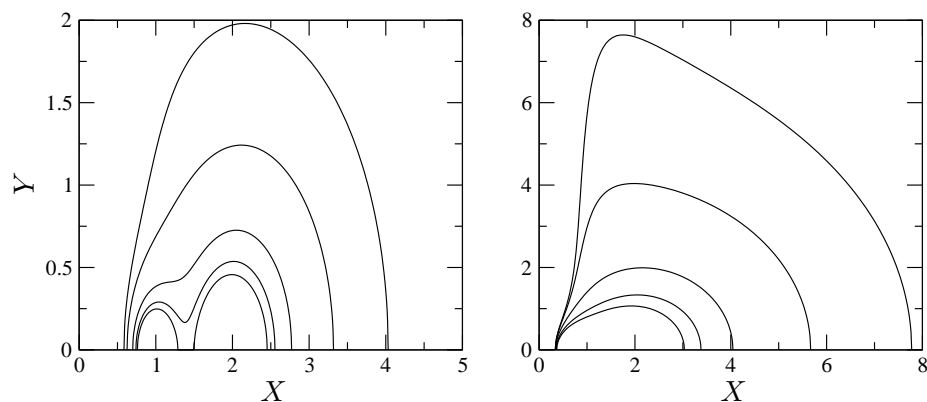
Fig. 1. Critical horizon for exponential correlations and $\{\lambda_i\} = \{1, 2\}$. The horizon is symmetric about the X axis; only upper part is shown. Left: $r = 0.1$ and $\tau = 0, 1, 2, 5$ from the inner to the outer horizon. Right: for $r = 0.5$ and $\tau = 0, 1, 2, 5$. Deviations from the shape expected in case of $\boldsymbol{A} = \boldsymbol{1}$ grow while the ratio $r/\sinh(1/\tau)$ increases.
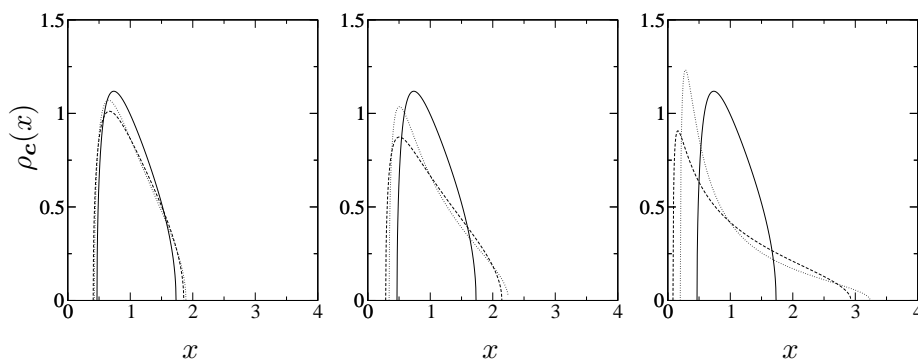

Fig. 2. Eigenvalues densities $\rho_{\boldsymbol{c}}(x)$ for pure Wishart $\boldsymbol{C} = \boldsymbol{A} = \boldsymbol{1}$ with fixed $r = 0.1$ (solid line), $\boldsymbol{C} = \boldsymbol{1}, r = 0.1$ and exponential correlations (21) (dotted line) and for pure Wishart with modified $r = 0.1 \cdot \coth(1/\tau)$ (dashed line) for different τ: $\tau = 1$ (left picture), $\tau = 2$ (middle picture), $\tau = 5$ (right picture). The distributions represented by dashed and dotted line behave similarly. In practice, when one reconstructs them only from one set of eigenvalues, they can be easily mixed up.

Consider now a practical example. In the previous paper [1] we discussed the evolution of the eigenvalue density of the experimental covariance matrix $\boldsymbol{c}$ with the number of independent measurements for $N = 18$ eigenvalues, obtained from data for daily returns of 18 stocks on the Polish Stock Market. Here we will discuss how the spectrum changes in case of correlated

returns as for example happens in short time horizons. We will use the same eigenvalues as before [1]. In the Fig. 3, $\rho_{\boldsymbol{c}}$ is shown for the three cases: for $r = 18/255$ without correlations ($\tau = 0$), for $r = 18/255$ and $\tau = 10$, and finally for $r = 10 \cdot 18/255$ and $\tau = 0$. We see that the first case deviates very much from the two remaining ones. Comparing the second and the third case we see that they follow the same trends. Technically in the second example one has ten times more data per degree of freedom but because the correlation time is equal to ten this means that roughly only every tenth data point introduces a new information. Therefore intuitively the second and the third case have a similar statistical content. Indeed a quick look at Eq. (22) shows that if one approximates the contribution from the square root by unity neglecting the term proportional to r^2 then this equation will assume the same form as Eq. (8) with an effectively rescaled parameter r: $r \to r \cdot \coth(1/10) \approx 10r$. This approximation is legitimate only if $r/\sinh(1/\tau) \ll 1$ as in the discussed example.

A similar observation can be made in a general case of arbitrary correlations $\boldsymbol{A}$. Consider the map (6) in case of small $r \ll 1$. Assuming that the
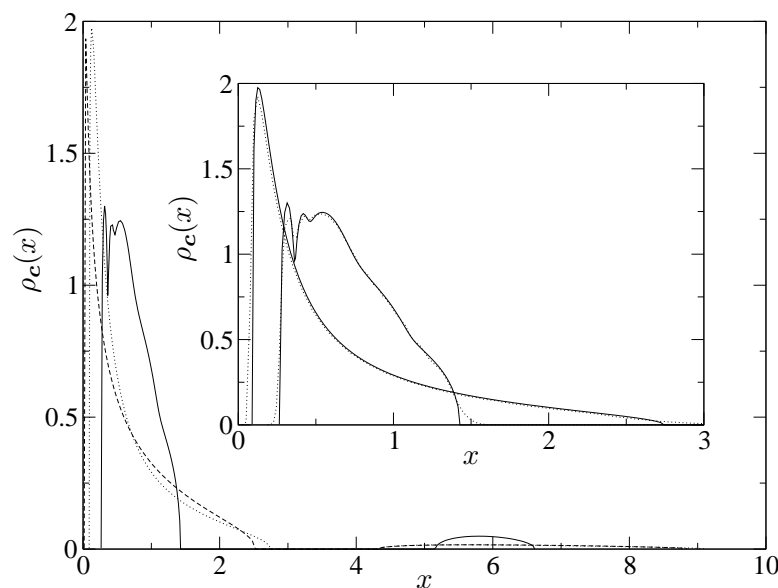

Fig. 3. The plot of $\rho_{\boldsymbol{c}}(x)$ for $N = 18$ eigenvalues of $\boldsymbol{C}$ taken from Polish Stock Market. Solid: $r = 18/255, \tau = 0$, dotted: $r = 18/255, \tau = 10$, dashed: $r = 180/255, \tau = 0$. Inset: the "bulk" of spectra for $r = 18/255$ and $\tau = 0, 10$ calculated (solid line) and found experimentally (dotted line) for sample of 3×10^5 Wishart matrices of size $N = 18$ generated by a Monte-Carlo procedure.

radius of the horizon is of order $\sqrt{r}$ as in case without correlations, from (9) it follows that $|rM_{\boldsymbol{C}}(Z)| \approx \sqrt{r}$ on the horizon. We can invert $M_{\boldsymbol{A}}(Z')$ for small Z':

$$M_{\boldsymbol{A}}^{-1}(Z') = M_{\boldsymbol{A}1} Z'^{-1} \left(1 + \mu_1 Z' + \mu_2 Z'^2 + \dots\right), \qquad (23)$$

where the coefficients of the series are expressed by the moments [8]:

$$\mu_1 = \frac{M_{\boldsymbol{A}2}}{(M_{\boldsymbol{A}1})^2}, \quad \mu_2 = \frac{M_{\boldsymbol{A}3} M_{\boldsymbol{A}1} - (M_{\boldsymbol{A}2})^2}{(M_{\boldsymbol{A}1})^4}, \quad \dots. \qquad (24)$$

Then the Eq. (6) takes the form:

$$z = M_{\boldsymbol{A}1} Z \left(1 + \mu_1 r M_{\boldsymbol{C}}(Z) + \mu_2 r^2 M_{\boldsymbol{C}}^2(Z) + \dots\right). \qquad (25)$$

The multiplicative factor $M_{\boldsymbol{A}1}$ merely redefines z and does not affect the map $z = z(Z)$. An important difference in comparison with Eq. (8) is the change of the coefficient at the linear term in r which tells us that for sufficiently small r the map (25) can be viewed as (8) but with of a modified parameter r: $r \to r \cdot \mu_1 = r M_{\boldsymbol{A}2}/(M_{\boldsymbol{A}1})^2$.
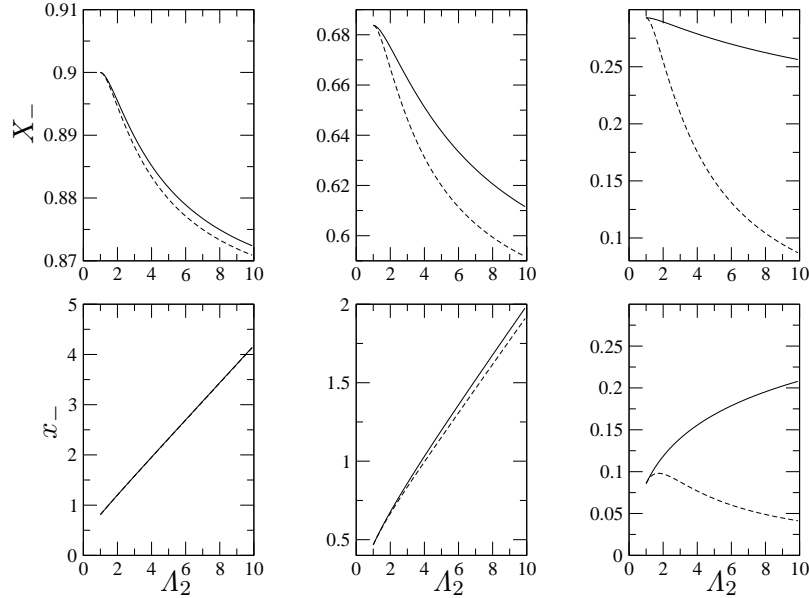

Fig. 4. Top: the position of left border X_- of the map $z = z(Z)$ for $\boldsymbol{C} = \boldsymbol{1}$ and $\{\Lambda_\alpha\} = \{1, \Lambda_2\}$ (solid line) and pure Wishart $\boldsymbol{C} = \boldsymbol{A} = \boldsymbol{1}$ with $r' = r\mu_1(\Lambda_2)$ (dashed line), from the left: $r = 0.01, 0.1, 0.5$. Bottom: the same for the left border x_- of spectrum $\rho_{\boldsymbol{c}}(x)$ with additionally rescaled x axis: $x \to x \cdot M_{\boldsymbol{A}1}$ for the Wishart case. The deviations from the rescaled Wishart spectrum become significant for $r > 0.1$.

To illustrate this, let us consider an example. Take $C = 1$ and A having two eigenvalues one of which being $\Lambda_1 = 1$ and the other Λ_2 being a free parameter. Additionally assume that the two eigenvalues have the same multiplicities and hence $p_1 = p_2 = 1/2$. The model looks somewhat artificial but it well illustrates a feature which is quite general.

In the upper part of Fig. 4 we compare positions of the left border X_- of the critical horizon (6) calculated in two different ways: numerically for different r, and analytically for the Wishart model without correlations with an effective "rectangularity" parameter $r' = \mu_1 \cdot r$, which gives $X_- = 1 - \sqrt{r'}$ where $\mu_1 = 2(1 + \Lambda_2^2)/(1 + \Lambda_2)^2$. The analogous comparison is made for the position of left border x_- of the eigenvalue density function $\rho_c(x)$ in the bottom of Fig. 4. Here we rescale additionally axes: $x \to x \cdot M_{A1}, y \to y/M_{A1}$ with the factor $M_{A1} = (1 + \Lambda_2)/2$ as in Eq. (25).

The corresponding eigenvalue distributions of the empirical covariance matrix c for these two cases for $r = 0.1$ are shown in Fig. 5. One sees an excellent agreement between them. This means that indeed for sufficiently small r the only influence of A on the spectrum of c is an effective change of r and rescaling the axes.

Let us shortly summarize. Using the relation between the moments generating functions (6) (or equivalently between the resolvents) we have shown how to effectively compute the eigenvalue spectrum of the empirically deter-
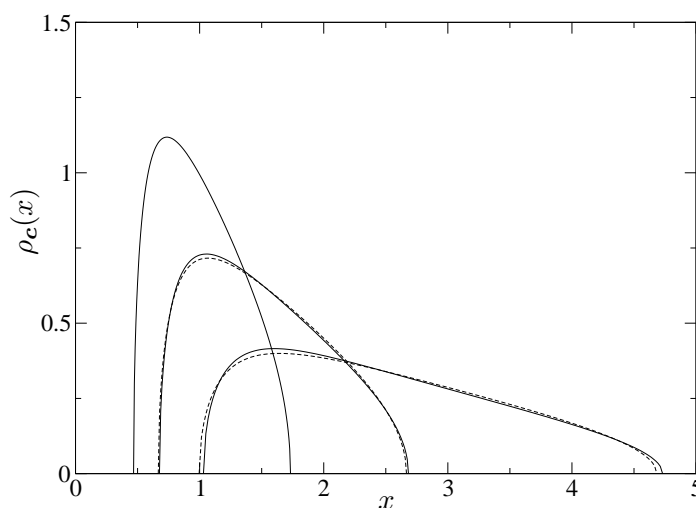

Fig. 5. The spectra for $r = 0.1, C = 1$ and A having two eigenvalues $\{1, \Lambda_2\}$ (solid line), and for rescaled Wishart (dashed line): $r \to r\mu_1, x \to x \cdot M_{A1}, y \to y/M_{A1}$. From the left to the right: $\Lambda_2 = 1, 2, 4$.

mined covariance matrix for given correlations, even in the case of correlated measurements. As an example of the application of the method we have demonstrated the influence of the exponential correlations between measurements on the eigenvalue spectrum of the covariance matrix calculated for stocks' logarithmic returns. We have argued that in the limit of the large number of samples that is for $T \gg N$, or equivalently for $r = N/T \ll 1$, the eigenvalue density of the empirical covariance matrix can be approximated by the eigenvalue density for a reduced number of uncorrelated samples, with the reduction factor being approximately inversely proportional to the correlation time for the original correlated samples.

REFERENCES

[1] Z. Burda, A. Görlich, J. Jurkiewicz, B. Waclaw, `cond-mat/0508341`.

[2] V.A. Marčenko, L.A. Pastur, *Math. USSR-Sb.* **1**, 457 (1967).

[3] Z.D. Bai, J.W. Silverstein, *J. Multivariate Anal.* **54**, 175 (1995).

[4] S.I. Choi, J.W. Silverstein, *J. Multivariate Anal.* **54**, 295 (1995).

[5] R. Müller, *IEEE Trans. Information Theory*, **48**, 2495 (2002).

[6] S.E. Skipetrov, *Phys. Rev.* **E67**, 036621 (2003).

[7] J.P. Bouchaud, P. Cizeau, L. Laloux, M. Potters, *Phys. Rev. Lett.* **83**, 1467 (1999).

[8] Z. Burda, J. Jurkiewicz, B. Waclaw, *Phys. Rev.* **E71**, 026111 (2005).

[9] S.H. Simon, A.L. Moustakas, *Phys. Rev.* **E69**, 065101 (2004).

[10] J. Wishart, *Biometrika* **A20**, 32 (1928).

[11] J. Feinberg, A. Zee, *J. Stat. Phys.* **87**, 473 (1997).

[12] P.P. Mitra, A.M. Sengupta, *Phys. Rev.* **E60**, 3389 (1999).

[13] Z. Burda, A. Görlich, A. Jarosz, J. Jurkiewicz, *Physica A* **343**, 295 (2004).